



HAL
open science

Experimental comparison between different configurations of PCM based heat sinks for cooling electronic components

Salma Gharbi, Souad Harmand, Sadok Ben Jabrallah

► **To cite this version:**

Salma Gharbi, Souad Harmand, Sadok Ben Jabrallah. Experimental comparison between different configurations of PCM based heat sinks for cooling electronic components. Applied Thermal Engineering, 2015, 87, pp.454-462. 10.1016/j.applthermaleng.2015.05.024 . hal-03448604

HAL Id: hal-03448604

<https://uphf.hal.science/hal-03448604v1>

Submitted on 18 Dec 2024

HAL is a multi-disciplinary open access archive for the deposit and dissemination of scientific research documents, whether they are published or not. The documents may come from teaching and research institutions in France or abroad, or from public or private research centers.

L'archive ouverte pluridisciplinaire **HAL**, est destinée au dépôt et à la diffusion de documents scientifiques de niveau recherche, publiés ou non, émanant des établissements d'enseignement et de recherche français ou étrangers, des laboratoires publics ou privés.

Experimental comparison between different configurations of PCM based heat sinks for cooling electronic components

Salma Gharbi ^{a,*}, Souad Harmand ^b, Sadok Ben Jabrallah ^a

^a University of Carthage, Science Faculty of Bizerte, 7021 Bizerte, Tunisia

^b University Lille Nord de France, F-59000 Lille, UVHC, TEMPO, F-59300 Valenciennes, France

H I G H L I G H T S

- Study on thermal performance of different PCM based heat sink in electronic cooling.
- Examination of heat transfer mechanism into heat sink for different conditions.
- Graphite matrix shows more efficiency than silicon.
- Inclusion PCM can reduce temperature increasing.
- Heat sink with longer well spaced fins can extend longer the critical time.

Keywords:

Phase change material
Heat sink
Cooling electronic components
Fins
Porous matrix

A b s t r a c t

The thermal control of electronic components is aimed at ensuring their use in a temperature range compatible with their performances. This paper presents an experimental study of the behavior of phase change materials (PCMs) as the cooling system for electronic devices. Four configurations are used to control the increase in the system temperature: pure PCM, PCM in a silicone matrix, PCM in a graphite matrix and pure PCM in a system of fins. Thermo-physical properties of different PCMs are determined and found to be desirable for application in this study. Solid liquid interface visualization and temperature evolution are employed to understand the mechanism of heat transfer during the different stages. Results indicated that the inclusion of PCM can lower component increase temperature and extends twice the critical time of the heat sink. The use of Graphite matrix filled by PCM showed more improvement on system thermal performance than silicon matrix. Also, for the same fraction of copper, it was found that incorporating long copper fins with suitable spacing into PCM, can enhance heat distribution into PCM leading to longer remain component temperature below the critical limit. This work therefore shows that the combination of PCM and long, well-spaced fins presents an effective means for thermal control of electronic devices.

1. Introduction

Thanks to their high heat storage capacity and isothermal behavior during melting and solidification, phase change materials are increasingly attractive in recent years. These materials can be employed in many applications such as thermal regulation of building, cooling electronic devices, heat storage and textile. For this purpose, many authors focused attention on their behavior in last decades. C. Gau et al. [1] analyzed the effect of natural

convection on interface transition and heat transfer during melting from below and solidification from above for a pure PCM in a rectangular enclosure. Benard convection cells were observed during melting. Also, it was found that the presence of natural convection increases the melting rate. More recently, H. Shoukhamand et al. [2] explored experimentally the melting process in a rectangular thermal storage unit heated from one side. They visualized the front evolution during solid–liquid phase change process. The dominance of heat conduction during early stage of melting, followed by dominance of convection heat transfer at later times were observed.

B. Kamkari et al. [3] studied the dynamic thermal behavior of phase change material (PCM) melting in a rectangular enclosure

* Corresponding author. Tel.: +33 752752945.

E-mail address: sallema0208@live.com (S. Gharbi).

Nomenclature

C_p	specific heat capacity, $\text{kJ kg}^{-1} \text{K}^{-1}$
G	thermal conductance, W K^{-1}
k	thermal conductivity, $\text{W m}^{-1} \text{K}^{-1}$
L_m	melting heat, kJ kg^{-1}
PCM	phase change material
T	temperature, K
t	time, s
t_c	critical time, s
$t_{c\text{ref}}$	critical time of reference configuration, s
$t_{c\text{conf}}$	critical time of the configuration, s
V	dynamic viscosity, Pa s^{-1}
ρ	density, kg m^{-3}
ϕ	power, W
τ	improvement rate of critical times
amb	ambient
c	critical
cr	crystallization
l	liquid
m	melting
s	solid

heated isothermally from one side at various inclination angles. It was found that the horizontal enclosure had more enhancement heat transfer than vertical enclosure. K. El Omari et al. [4] analyzed the impact of different enclosure geometries filled with thermal conductivity enhanced PCM. It was observed that the configuration with a portion of PCM placed above the cooled surface provided the best efficiency.

In electronic applications, using PCMs for thermal control of electronic devices can offer a great advantage by stabilizing the temperature for a long period and improving device longevity. Several studies have been conducted to investigate the use of PCM in cooling of electronic devices. F.L. Tan et al. [5] investigated experimentally a heat storage unit filled by PCM for cooling of portable hand held electronic devices. It was revealed that the use of PCM can stabilize the system temperature under allowable temperature of 50°C for 2 h of transient operations of the device. R. Kandasamy et al. [6] studied numerically and experimentally the use of PCM based heat sink. They evaluated the effect of power input, orientation of package, and various melting/solidification times under cyclic steady conditions. It was concluded that using PCM-based heat sinks improve the thermal performance of electronic component during intermittent use.

However, PCMs suffer from a low thermal conductivity which limits their efficiency. To overcome this problem, some heat transfer enhancement techniques were employed, such as micro-encapsulation of PCM, dispersed high thermal conductivity particles, incorporating porous matrix and extending fins inside the PCM. O. Mesalhy et al. [7] conducted a numerical study of the melting process inside high thermal conductive, porous matrices saturated with PCM. It was reported that the presence of the matrix has a great effect on heat transfer. L. Jian-Feng et al. [8] prepared a composite PCM by absorbing paraffin into expanded graphite. It was noted that using the composite PCM can protect the electronic device from the shock of high heat flux and keep its operating stability. It was also showed that the apparent heat transfer coefficients in the heat sink with PCM are 1.36–2.98 times larger than those in the heat sink without PCM.

Numerous researchers have focused their attention on using extending fins inside PCM. S.F. Hosseinzadeh et al. [9] conducted an experimental and numerical study on PCM stored in finned enclosure for cooling application. The effects of various parameters such as power levels, number of fins, fin height and fin thickness on the heat sink performance were evaluated. It was showed that increasing the number of fins and fin height improve overall thermal performance, while increasing the fin thickness presented a slight improvement. S. Mahmoud et al. [10] examined experimentally the thermal performance of PCM confined between different configurations of inserts. It was indicated that increasing fin number for the heat sink with parallel/crossed fins can enhance heat transfer leading to reduce peak temperatures. Moreover, several authors carried out on melting process into PCM with partial fins. Lacroix and Benmadda [11] carried out numerical studies on PCM filling a rectangular enclosure with horizontal fins heated from one side. It was concluded that the natural convection effects was improved when the PCM thickness within the fins was large. Huang et al. [12] performed a numerical and experimental study on thermal regulation of photovoltaic system by inserting partial horizontal fins. Authors noted an improvement in temperature regulation. Yet, increasing number of fins can decrease regulation effect by limiting convection flow in the melted PCM. L. Tan et al. [13] conducted a numerical investigation of PCM melting in a finned rectangular enclosure. Four different fin shape configuration: straight fin, T-shape fin, Y-shape fin and cross-shape fin were compared to eight straight fins configuration. It was concluded a marginal improvement in heat transfer.

In addition to these experimental and numerical studies on the use of PCM in order to improve the thermal protection of electronic equipment, several researchers were interested by conducting numerical studies to better optimize the geometry of cooling systems to improve their performance and cost. In this context, M.R. Hajmohammadi et al. investigated different configurations shape of highly conductive pathways such as fork [14] and Phi and Psi shape [15] and they concluded that these configurations operated better than X-shaped configurations. Moreover, as a convective system, H. Najafi et al. [16] investigated the optimization of a plate and fin heat exchanger PFHE using genetic Algorithm considering multi-objective for maximizing the total heat transfer rate and minimizing the total cost of the system. M.R. Hajmohammadi et al. [17] analysed the optimal thickness of plate for reducing the excess temperature of iso-heat flux heat sources cooled by laminar forced convection flow. For radiation systems, M.R. Hajmohammadi et al. [18] incorporated the radiation with convection heat transfer in constructal design of a T–Y shaped assembly of fins and performed a parametric study. As indicated before [15–18], the constructal design is used by many researchers in order to optimize cost and efficiency of heat transfer.

From the above literature, it was seen that there are few experimental studies focused on maximizing the time at which the heat sink base achieves a critical temperature and visualizing of solid liquid interface and temperature evolution in different PCMs heat sinks. For this purpose, the aim of this work is to experimentally examine the thermal performance of different PCM based heat sinks as follows: pure PCM, PCM in a silicon matrix, PCM in a graphite matrix and pure PCM in a fin system during the melting and solidification processes to extend critical time of system below a critical temperature. Photographic observation of the solid liquid interface evolution during melting allows a good understanding of heat transfer mechanism inside the enclosure. This better understanding will improve the performance and design of the system and will serve as a starting point for future numerical optimization study.

Table 1
Composition of PCMs (PCM/silicon, PCM/graphite).

Composition	PCM/silicon	PCM/graphite
Additives	Particle of copper to improve thermal conductivity of the formulation Boron nitride and graphite for fire foam formulation	Polymer to improve the flexibility of the formulation
Aging	After 3000 cycles, properties change <1%.	After 3000 cycles, properties change <1%.

2. Experimental apparatus and procedure

2.1. Measurement of thermophysical properties

The PCM used in this study was a commercial product, plastic paraffin. The description of the two composite PCMs (PCM/silicone matrix and PCM/graphite matrix) is mentioned in Table 1. It was observed that these materials are suitable for application due to their melting temperature, which is below critical temperature (60 °C). Furthermore, these materials are suitable because of their favorable characteristics such as non-toxicity and chemical stability even after 3000 cycles. Thermal properties of all PCMs are described below in Table 2.

Thermal conductivity measurements were made by FP2C based on the hot wire method. Thermal measurements were performed at two temperature levels, at 30 °C (the solid phase) and at 70 °C (the liquid phase). Table 3 shows the value of thermal conductivity at each temperature. The accuracy of thermal conductivity measurements is 5%.

Specific heat capacity measurements were determined by differential scanning calorimetry (DSC) using the Mettler Toledo Star DSC 1. The DSC thermal analyses were performed with a heating rate of 20 °C/min in the temperature range from 20 to 70 °C. For the PCM/porous matrix, equivalent specific heat capacity is measured by the DSC. Fig. 2 present the respective variations of the specific heat capacities of the paraffin (a) and the PCM/porous matrices (b) (Silicon and graphite).

The latent heat and the melting and crystallization temperature measurements were also determined by differential scanning calorimetry (DSC). During the first heating, an endothermic phenomenon occurred at 53 °C and repeated at 51 °C during second heating. During cooling, an exothermic phenomenon occurred at 48 °C. Therefore, melting and crystallization temperatures were determined ($T_m = 51.75$ °C and $T_{cr} = 47.84$ °C). The latent heat of the solid–liquid phase change was calculated by numerical integration of the area under the peak of the DSC curve. Fig. 3 shows the DSC heating thermogram of paraffin (138.23 J g⁻¹).

The dynamic viscosity measurement was determined by a viscoanalyzer type DMA Metravib VA 4000 for a temperature range of 20–70 °C, with a heating rate of 2 °C/min. Fig. 4 shows the variation of the dynamic viscosity of paraffin.

2.2. Apparatus and instrumentation

A schematic diagram of the apparatus used in this study is shown in Fig. 5. It consists mainly of a PCM container, a heater, a

power supply, a temperature data logger, a personal computer and a digital camera.

Fig. 6 shows the schematic representation of the cooling system. This system consists of a PCM container with inside dimensions of (51.5 * 25.5 * 16.5) mm³. The right wall of the enclosure was closed by a copper slab with dimensions of (38.5 * 5.5 * 16) mm³, contacting a heater with the same dimensions, joined to a power supply (Heinzinger LNG 32-15). The other walls of the enclosure were made of 4 mm thick (front and left faces), 12 mm thick (top and bottom faces) and 15 mm thick rear faces, of transparent Plexiglas sheets to allow for the photographic observation of the melting process. For further insulation, the heater was insulated with polystyrene.

Five thermocouples with a calibrated accuracy of ±0.5 °C were placed in different locations to measure the transient temperature distribution. Thermocouple locations included three units at the inner copper slab face, one unit between the heater and copper slab and a final unit outside to measure the ambient temperature. All thermocouples are connected to the computer through a data logger to record temperature. A digital camera (Nikon D90) was used to visually record the melting front evolution.

2.3. Experimental procedure

Each experiment was composed of two phases: the temperature rise and melting of the PCM phase followed by the phase of solidification of the PCM by removing the heater until the temperature returns to its initial value. To visualize the melting front evolution, photographs are taken every 5 min. The temperatures of the PCM at the specified locations were logged every 1 s. Every experiment was performed twice to verify their repeatability. The experiments in this study were conducted using a heating system with a power of (4 W) and at an ambient temperature of (22 °C ± 1 °C). Table 4 shows all experimental configurations used.

3. Results

3.1. Photographic observation of melting front of different PCMs

To understand heat transfer mechanisms occurring during phase change process in the enclosure, it was recommended to investigate different melting front positions for different PCMs (pure PCM and PCM/silicone matrix). These were presented in the photographs in Fig. 7 for both the horizontal and the vertical positions at two different times (60 and 120 min). In these photographs, the set of points represent the melting front for the two

Table 2
Thermo-physical properties of PCMs and copper.

Materials	Thermal conductivity (W m ⁻¹ K ⁻¹)	Specific heat capacity (kJ kg ⁻¹ K ⁻¹)	Density (kg/m ³)	Melting and crystallization temperature(°C)	Latent heat (kJ/kg)
Copper	401	0.385	8933	–	–
Plastic paraffin	0.234(s) 0.164(l)	2.710(s) (25 °C) 4.640(l) (65 °C)	900	51.75(m) 47.84(cr)	138.23
PCM/silicon matrix	1	f(T) (Fig. 4)	1200	37	188
PCM/graphite matrix	1	f(T) (Fig. 4)	900	37	188

Table 3

Thermal conductivity of paraffin at two temperature levels (30 °C and 70 °C).

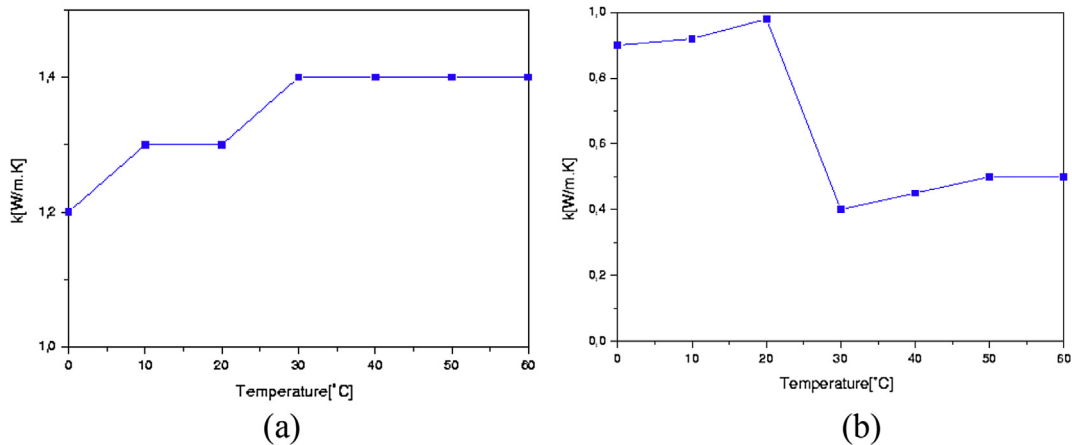
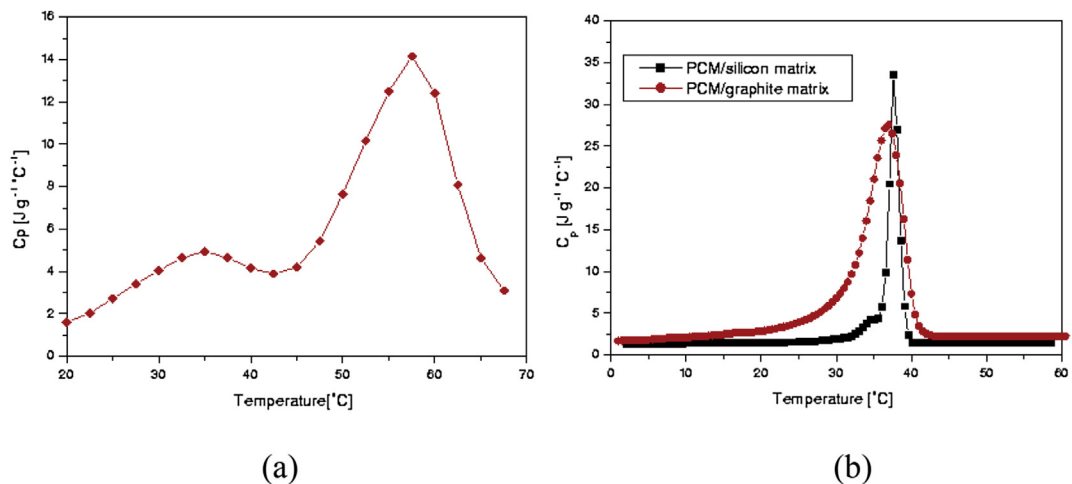
Experiment	Thermal conductivity ($\text{W m}^{-1} \text{K}^{-1}$)	
	Paraffin at 30 °C	Paraffin at 70 °C
1	0.238	0.167
2	0.231	0.163
3	0.231	0.164
4	0.231	0.164
5	0.239	0.164
Average	0.234	0.164
Standard deviation	0.004	0.001

cases and the darker area presents the liquid region. At $t = 60$ min, it can be clearly seen from picture a melting front parallel to the hot wall announcing that conduction was the predominated mode. It was also observed that the melting front is not straight because the copper slab was placed in the middle of the enclosure face. The composite material had a more advanced melting front than the paraffin. This result can be explained by the different thermal properties of the PCM/silicon matrix ($T_m = 37$ °C, $k = 1$ W/m K) and of the Paraffin ($T_m = 51.75$ °C, $k = 0.234$ W/m K). At the vertical position, there is no important difference compared to horizontal position because the mode of heat transfer is yet predominated by conduction in the two cases. As time progressed ($t = 120$ min), it

was noted that the (PCM/silicon matrix) melting front remained parallel to the heated wall which can be explained by the fact that silicon matrix prohibited PCM to move while the paraffin melting front was deformed after the convective cell appearance in the liquid area. In the case of the vertical position, the (PCM/silicon matrix) presented the same mode, whereas the paraffin presented a deformed front indicating a more pronounced melting on the top part of the enclosure. This is due to the importance of the convective movement.

3.2. Effect of the nature of PCM on thermal performance

Fig. 8 presents the temperature variation measured at the surface of copper slab for three configurations (1, 2 and 3) at two positions and during two phases (charge and discharge). Using a porous matrix is advantageous to keep melted PCM in pores as a result of capillary forces. As shown in Fig. 8, the same temperature profile for the three cases (temperature increase followed by a permanent regime then a temperature decrease until reaching the initial value) was observed. The fastest temperature rise was observed in the first configuration, followed by the PCM/silicon matrix and, finally, in PCM/graphite matrix. This classification indicates also the order of the global conductivity of each configuration. It was noted that a decreased slope for the PCM/graphite

**Fig. 1.** Variation of thermal conductivity of (a) PCM/graphite matrix and; (b) PCM/silicon matrix versus temperature.**Fig. 2.** Variation of specific heat capacity of (a) paraffin; (b) PCM/graphite and PCM/silicon versus temperature.

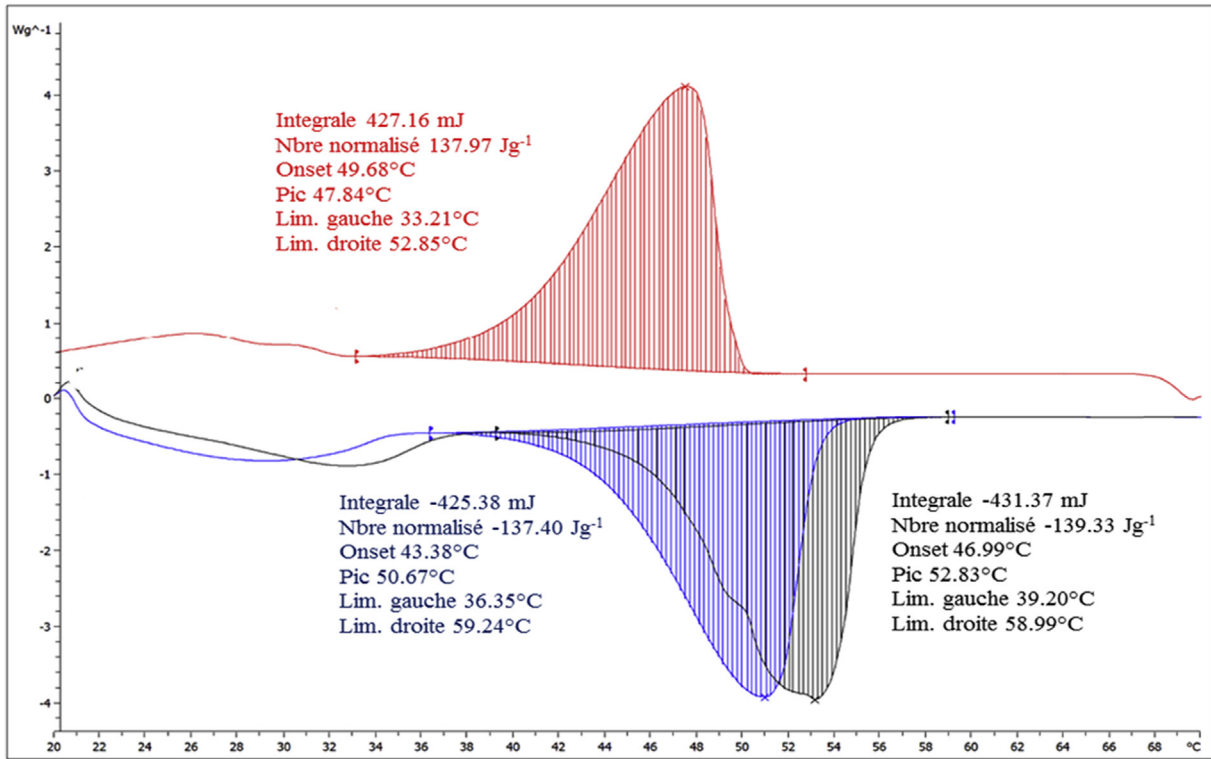


Fig. 3. DSC heating thermogram of paraffin.

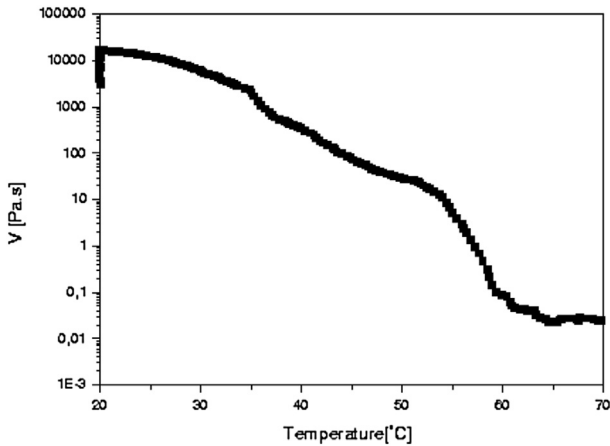


Fig. 4. Variation of the dynamic viscosity of paraffin versus temperature.

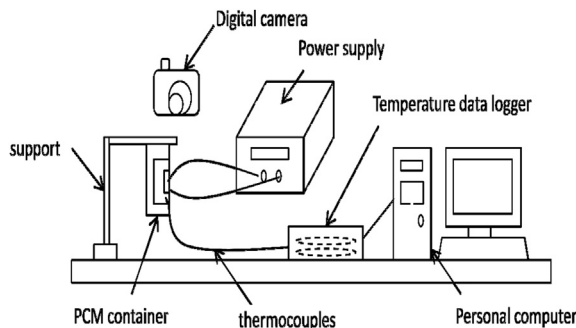


Fig. 5. Schematic diagram of the experimental apparatus.

occurred at 1700 s then at 6600 s. These slope changes can be explained by the phase change melting: the beginning for the first and the end for the second.

This phenomenon is not readable for the silicon case and this can be explained by the difference in the specifications of the two matrixes. . In steady state, the temperature reached by 1st configuration, 2nd and 3rd were respectively around 100 °C, 94 °C and 73 °C. The heat storage capacity of the PCM (Fig. 2(a)) and the different dependence of the thermal conductivity with temperature for two different formulations (Fig. 1) can explain this shift. It is notable that in the second part (discharge), a similar pattern

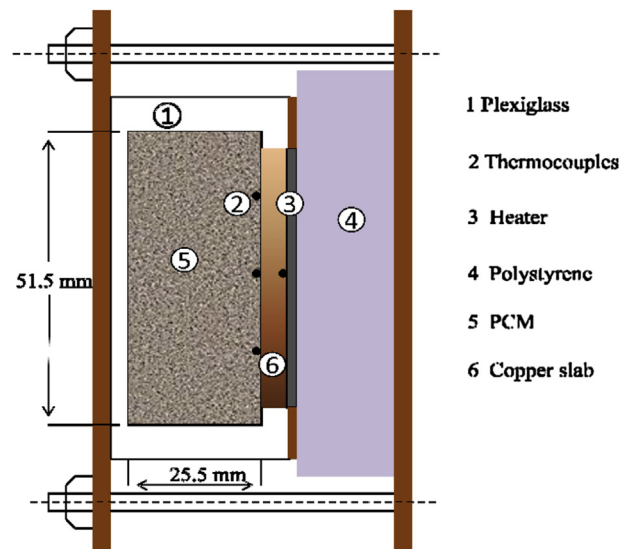
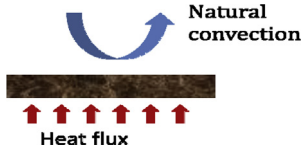
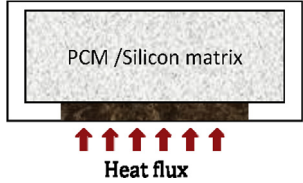
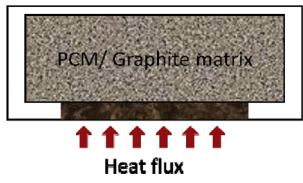
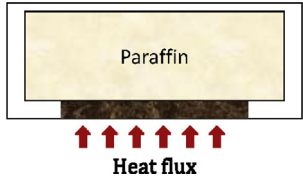
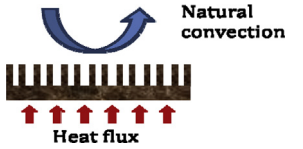
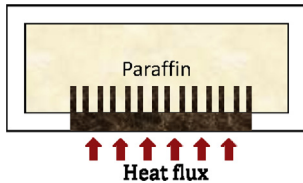
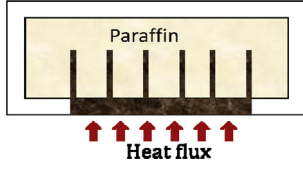


Fig. 6. Schematic representation of cooling system.

Table 4
Description of different configurations used in this study.

Configurations	Characteristic	Schema
1	Copper slab	
2	Copper slab + PCM/silicon matrix	
3	Copper slab + PCM/graphite matrix	
4	Copper slab + Paraffin	
5	Copper slab with 14 fins	
6	Copper slab with 14 fins + Paraffin	
7	Copper slab with 6 fins + Paraffin	

occurred for both formulations with a change in slope at the time of 16,200 s, indicating the beginning of solidification.

3.3. Effect of fins addition on thermal performance

In Fig. 9, the temperature profile measured at the surface of the copper slab was presented for four configurations (1, 4, 5 and 6) at

horizontal position during charge phase. At first, it is clearly noted that temperature profile had different slopes. The fastest temperature rise was observed for the first configuration, followed by fifth then by fourth and, finally for sixth configuration. This difference can be explained by the increased exchange surface area and the high heat capacity storage of PCM. For configuration 4, it was noted a slope drop at 3,600 s occurred by transition from conductive to the convective regime in the melted region as shown in photographs (Fig. 10(a)). For configuration 6, a slope drop was observed at 1800 s then at 4300 s. This drop is illustrated in (Fig. 10(b)) and can be explained by the start of the PCM melting between the fins, and by the shift away of the melting front from fins indicating the appearance of the convective regime. By reaching the permanent regime, it was detected a gap around 20 °C between maximal temperatures (configuration 1 and 5) and around 10 °C between (configuration 4 and 5). A very small gap was seen between (configuration 4 and 6) which can be explained by the fact that moving away of melting front from fins, the PCM starts behaving as PCM with no addition (configuration 4).

3.4. Effect of fins arrangement

To examine the effects of fins arrangement, two copper slabs with different fins arrangement (configuration 6 and 7) (Table 5), having the same fraction of copper and varied simultaneously in length and number, were used.

3.5. Photographic observation of the melting front of different fins arrangement

In Fig. 11, the diverse positions of the melting front of the two configurations 6 and 7 were presented for two positions and at two different times (80 and 110 min). For this case, times are chosen different comparing with precedent case because the regime transition in these two configurations appears at different times. At $t = 80$ min, for the configuration 6, a faster melting of the PCM was observed in comparison with seventh one. The 6th configuration had a thin, fully melted PCM, layer between the fins, while the 7th configuration had more fin spacing with a thick layer of PCM that started to melt near the base side. This can be explained by the fact that better distribution of heat delays beginning of the melting. At the vertical position, the same behavior was observed because the conductive regime was the predominant for both cases. At $t = 110$ min, the melting front of the heat sink with 14 fins moved away from the fins surface area; therefore, the convective regime was established for both positions. Furthermore, for the heat sink with 6 fins, a purely conductive regime was started, leading to a corrugated melting front at fins tip. At vertical position, the 6th configuration presents a deformed melting front indicating the strength of convective cells leading to more melting in the top of enclosure while the 2nd shows yet the same behavior. In fact, the way of differently arranging fins enabled the control of the regime established in the cavity and the subsequent thermal performance.

3.6. Effect of fins arrangement on thermal performance

In Fig. 12, the temperature profile measured at the surface of the three configurations (4, 6 and 7) was presented for the horizontal position for both phases (charge and discharge). The change in the slope for the configurations (4 and 6) can be explained as early by the start of the phase change then by the onset of convective cells in liquid region. For the configuration 7, an inclined plateau is observed between 3600 s and 7400 s. Fig. 10(c) can explain this plateau, as found in the case of configuration 6. This configuration presents a longer phase change in comparison with previous

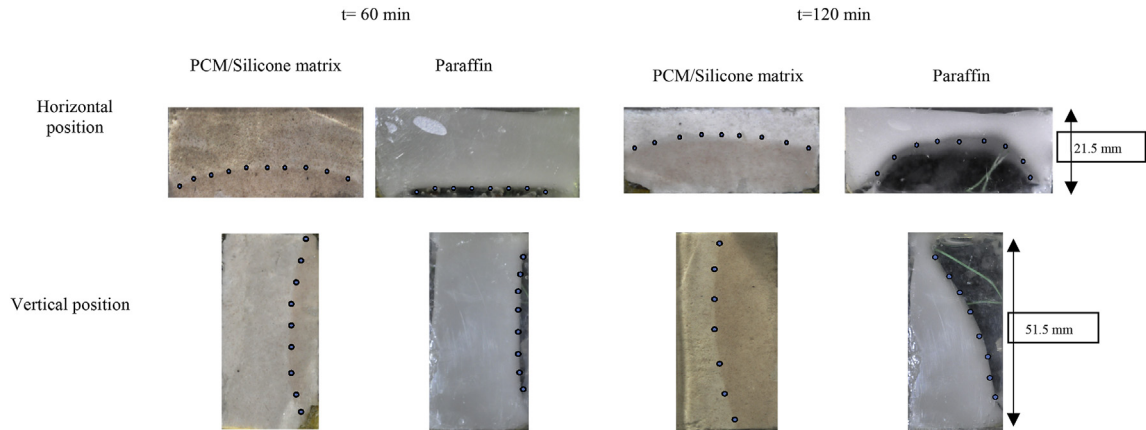


Fig. 7. Photographs of the melting front of two different PCMs (PCM/silicone matrix (left), paraffin (right)) at two positions and different times.

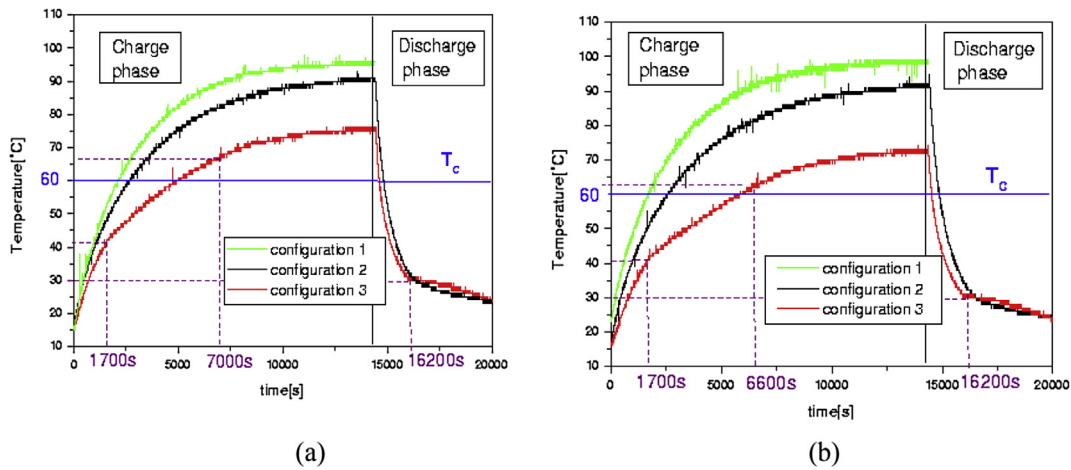


Fig. 8. Variation of temperature of the three configurations (1, 2 and 3) during two phases (charge and discharge) at two positions (a) vertical and (b) horizontal.

configuration (configuration 6) and can be justified by the different fin length. At steady state, it was detected that the heat sink with six fins dampened the increase in temperature and had 5 °C lower temperature in comparison with the heat sink with 14 fins. In fact, the increase in the length of the fins involved better heat distribution throughout the cavity filled by PCM. For the discharge phase, it was discovered that the two sinks behaved in the same manner;

this can be attributed to the conservation of the same fraction of copper fins. For the three curves, a decrease in the slope at 15,000 s was detected. This can be explained by the beginning of solidification. After this, between 15,000 and 18,000 s, the thermal inertia of the fins is behind the maintenance of a higher temperature at the beginning of the discharge phase for configurations 6 and 7. The use of the fins during the discharge phase shows no contribution compared to the single plate.

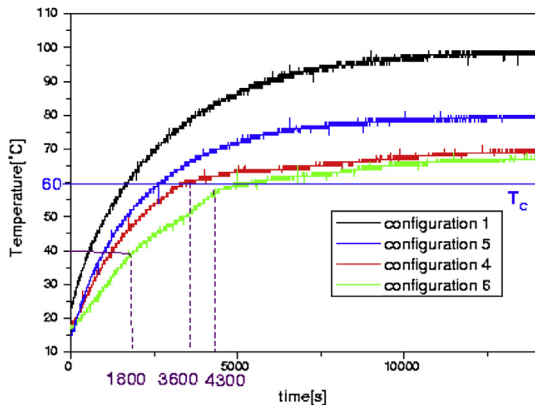


Fig. 9. Variation of temperature of the four configurations (1, 4, 5 and 6) during charge phase at the horizontal position.

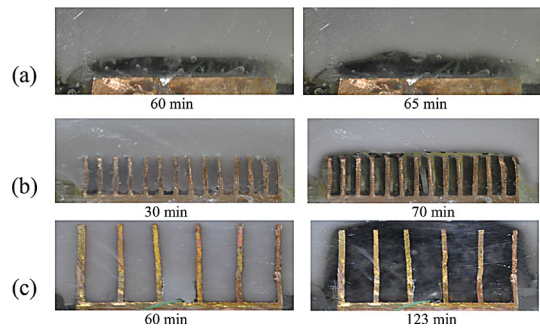
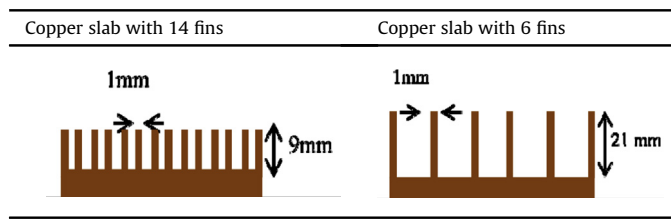


Fig. 10. Photographs of the melting front of different configurations (4, 6 and 7) at different times.

Table 5

Description of the two copper slabs with fins used in this study.



3.7. Comparison of critical time

Comparing the thermal performance of these configurations is based on the specificities of the application. In this particular application, maintaining the system temperature below a critical temperature (60 °C) for a sufficiently long period is critical. Therefore, the results are analyzed by comparing the critical time elapsed to reach the critical temperature. In Fig. 13(a), the critical time for all configurations at the horizontal position is presented. From Table 6 the improvement rate of the critical time for different configurations with respect to the reference configuration (configuration1) is shown. It may be noted that the configuration of PCM/graphite matrix appears more efficient compared to that of silicone in maintaining the temperature below 60 °C for a period more than three times that of the reference case (configuration 1). By introducing the PCM, the critical time for the two cases (copper slab with and without fins) was doubled. By adding fins, it was observed that the critical time was extended to one and a half for the two cases (with and without PCM). Although adding fins decreased the amount of PCM in the cavity, it allows the extension of critical time nearly six times longer than the reference configuration for the case of configuration 7. It can be concluded that the extension of system critical time also depends on the presence of PCM and the manner of fins distribution.

3.8. Comparison of thermal conductance

Fig. 13(b) illustrates the thermal conductance, G (Equation (1)), of the different configurations at the horizontal position and during the charge phase. G is the thermal conductance characteristic of the total heat exchange at the surface in a steady regime. From Fig. 13(b), it is noted that configuration 7 has the best conductance at the surface. Good heat transfer within the PCM and through the long fins can explain this result.

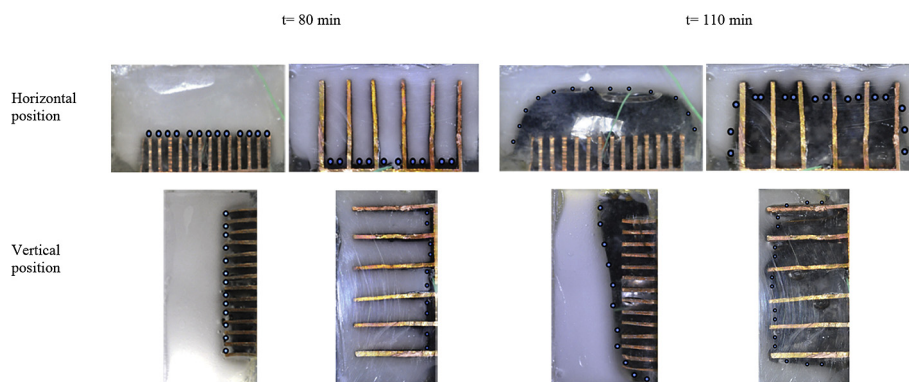


Fig. 11. Photographs of the melting front of the two different configurations (6 and 7) for two positions and at different times.

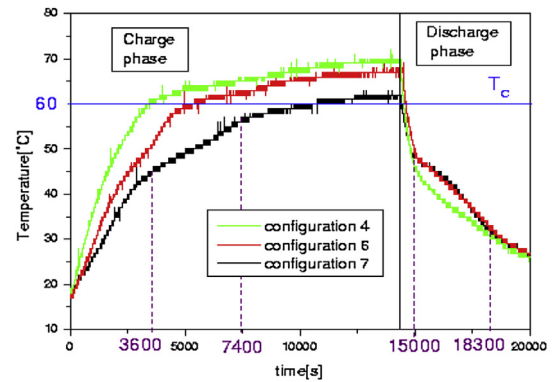


Fig. 12. Variation of temperature of the three configurations (4, 6 and 7) for two phases (charge and discharge) at horizontal position.

$$G = \frac{\phi}{T_{max} - T_{amb}} \quad (1)$$

4. Conclusions

The goal of this study was to determine the most thermally efficient configuration for controlling electronic devices, based on the critical time elapsed by the system to reach a critical temperature. Characterization of the thermal conductivity, phase change points, specific heat capacity and latent heat of fusion were performed. The comparison of the PCM behavior in different configurations was carried out to better understand the mechanism of heat transfer. The results show that:

- At different stages and positions, porous matrix prohibits PCM to move leading to the predomination of the conductive regime however pure PCM presents various behaviors.
- The inclusion of PCM extends twice the critical time of the heat sink.
- Graphite matrix allows more thermal control of system than silicon matrix.
- The use of fins indicates an important contribution during melting.
- For the same fraction of copper, it is advantageous to employ a copper slab with longer well spaced fins for a better thermal control of the system.
- The highest critical time (up to six times) and thermal conductance were observed for the heat sink with six fins.

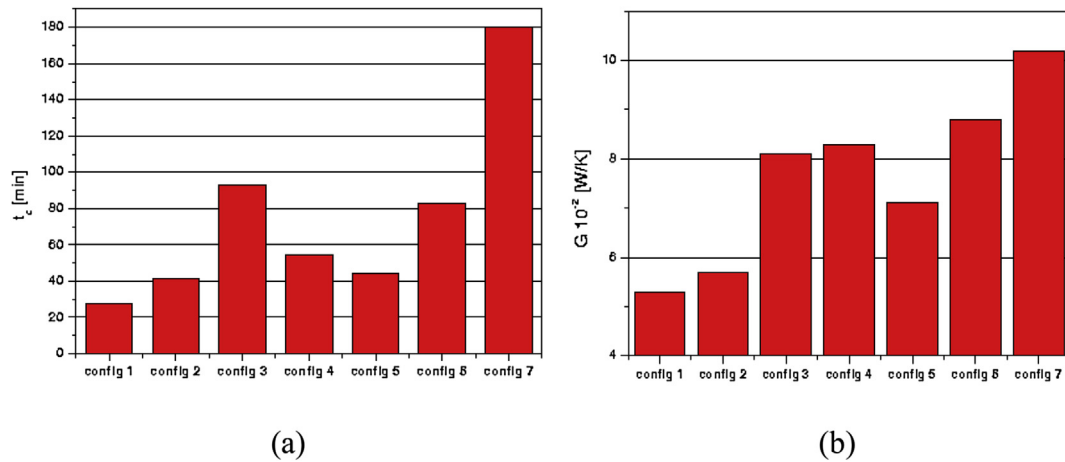


Fig. 13. Comparison of the critical time (a) and thermal conductance (b) at the surface of different configurations at the horizontal position during the charge phase.

Table 6
Improvement rate of the critical time for different configurations with respect to the reference configuration (configuration1).

Configuration	1	2	3	4	5	6	7
$\tau = (t_{c\text{conf}}/t_{c\text{ref}})$	1	1.5	3.4	2	1.6	3	6.5

References

- [1] C. Gau, R. Viscanta, Effect of natural convection on solidification from above and melting from below of a pure metal, *Int. Heat Mass Transf.* 28 (1985) 573–587.
- [2] H. Shokouhmand, B. Kamkari, Experimental investigation on melting heat transfer characteristics of lauric acid in a rectangular thermal storage unit, *Exp. Therm. Fluid Sci.* 50 (2013) 201–212.
- [3] B. Kamkari, H. Shokouhmand, F. Bruno, Experimental investigation of the effect of inclination angle on convection-driven melting of phase change material in a rectangular enclosure, *Int. J. Heat Mass Transf.* 72 (2014) 186–200.
- [4] K. El Omari, T. Kousksou, Y. Le Guer, Impact of shape of container on natural convection and melting inside enclosures used for passive cooling of electronic devices, *Appl. Therm. Eng.* 31 (2011) 3022–3035.
- [5] F.L. Tan, C.P. Tso, Cooling of mobile electronic devices using phase change materials, *Appl. Therm. Eng.* 24 (2004) 159–169.
- [6] R. Kandasamy, X. Wang, A.S. Mujumdar, Application of phase change materials in thermal management of electronics, *Appl. Therm. Eng.* 27 (2007) 2822–2832.
- [7] O. Mesalhy, K. Lafdi, A. Elgafy, K. Bowman, Numerical study for enhancing the thermal conductivity of phase change material (PCM) storage using high thermal conductivity porous matrix, *Energy Convers. Manag.* 46 (2005) 847–867.
- [8] L. Jian-Feng, Y. Hong-Wei, L. Wen-Yu, X. Zhong-Jie, S. Zheng-Zheng, X. Xiao-Jun, Ch. Sheng-Li, Numerical and experimental study on the heat transfer properties of the composite paraffin/expanded graphite phase change material, *Int. J. Heat Mass Transf.* 84 (2015) 237–244.
- [9] S.F. Hosseini, F.L. Tan, S.M. Moosania, Experimental and numerical studies on performance of PCM-based heat sink with different configurations of internal fins, *Appl. Therm. Eng.* 31 (2011) 3827–3838.
- [10] S. Mahmoud, A. Tang, C. Toh, R. AL-Dadah, S. Leung Soo, Experimental investigation of inserts configurations and PCM type on the thermal performance of PCM based heat sinks, *Appl. Energy* 112 (2013) 1349–1356.
- [11] M. Lacroix, M. Benmadda, Numerical simulation of natural convection-dominated melting and solidification from a finned vertical wall, *Numer. Heat Transf.* 31 (1997) 71–86.
- [12] M.J. Huang, P.C. Eames, B. Norton, Thermal regulation of building-integrated photovoltaics using phase change materials, *Int. J. Heat Mass Transf.* 47 (2004) 2715–2733.
- [13] L. Tan, Y. Kwok, A. Date, A. Akbarzadeh, Numerical analysis of natural convection effects in latent heat storage using different fin shapes, *Int. J. Energy Sci., School of Aerospace, Mechanical, Manufacturing Engineering, RMIT University Melbourne, Australia.*
- [14] M.R. Hajmohammadi, V. Alizadeh Abianeh, M. Moezzinajafabadi, M. Daneshi, Fork-shaped highly conductive pathways for maximum cooling in a heat generating piece, *Appl. Therm. Eng.* 61 (2013) 228–235.
- [15] M.R. Hajmohammadi, O. Joneydi Shariatzadeh, M. Moulod, S.S. Nourazar, Phi and Psi shaped conductive routes for improved cooling in a heat generating piece, *Int. J. Therm. Sci.* 77 (2014) 66–74.
- [16] H. Najafi, B. Najafi, P. Hoseinpoori, Energy and cost optimization of a plate and fin heat exchanger using genetic algorithm, *Appl. Therm. Eng.* 31 (2011) 1839–1847.
- [17] M.R. Hajmohammadi, M. Moulod, O. Joneydi Shariatzadeh, A. Campo, Effect of a thick plate on the excess temperature of iso-heat flux heat sources cooled by laminar forced convection flow, *Conjug. Anal. Numer. Heat Transf. Part A* 66 (2014) 205–216.
- [18] M.R. Hajmohammadi, S. Poozesh, R. Hosseini, Radiation effect on constructal design analysis of a T–Y-shaped assembly of fins, *J. Therm. Sci. Technol.* 7 (2012) 677–692.